Quantum Advantage Actor-Critic for Reinforcement Learning

Michael Kölle*, Mohamad Hgog*, Fabian Ritz, Philipp Altmann, Maximilian Zorn, Jonas Stein and Claudia Linnhoff-Popien
Institute of Informatics, LMU Munich, Munich, Germany

Keywords: Quantum Computing, Quantum Reinforcement Learning, Advantage Actor-Critic.

Abstract: Quantum computing offers efficient encapsulation of high-dimensional states. In this work, we propose a novel quantum reinforcement learning approach that combines the Advantage Actor-Critic algorithm with variational quantum circuits by substituting parts of the classical components. This approach addresses reinforcement learning's scalability concerns while maintaining high performance. We empirically test multiple quantum Advantage Actor-Critic configurations with the well known Cart Pole environment to evaluate our approach in control tasks with continuous state spaces. Our results indicate that the hybrid strategy of using either a quantum actor or quantum critic with classical post-processing yields a substantial performance increase compared to pure classical and pure quantum variants with similar parameter counts. They further reveal the limits of current quantum approaches due to the hardware constraints of noisy intermediate-scale quantum computers, suggesting further research to scale hybrid approaches for larger and more complex control tasks.

1 INTRODUCTION

Quantum computing (QC) promises to revolutionize problem-solving by exploiting quantum mechanics' unique properties, potentially outperforming classical computers in complex tasks such as quantum cryptography, quantum chemistry, and quantum optimization (Nielsen and Chuang, 2010; Preskill, 2018; Pirandola et al., 2020; Shor, 1997; Cao et al., 2019; Bauer et al., 2020; Dral, 2020; Farhi and Harrow, 2016; Cerezo et al., 2020; Farhi et al., 2014). This has spurred interest in quantum machine learning (QML), particularly in leveraging quantum interference for accelerated training and inference in machine learning models (Biamonte et al., 2017).

Reinforcement learning (RL) is a machine learning subfield focused on training agents to interact with an environment and learn from their experiences. RL has achieved remarkable success in applications such as game playing (e.g., AlphaGo (Silver et al., 2017)), robotics (Kober et al., 2013), and autonomous driving (You et al., 2017). However, the performance of classical RL algorithms is often limited by their sample inefficiency. This leads to slow convergence and requires a large number of interactions with the environment. Since quantum computing offers the efficient encapsulation of high-dimensional states as one of its significant benefits, recent research interest in quantum reinforcement learning (QRL) has emerged (Meyer et al., 2022b).

This work concentrates on the Advantage Actor-Critic (A2C) method, a well-established RL algorithm, in the context of QRL (Konda and Tsitsiklis, 1999; Mnih et al., 2016; Andrychowicz et al., 2021). We explore the application of variational quantum circuits (VQCs) in policy gradient methods like A2C, suitable for current noisy intermediate scale quantum (NISQ) computers (Preskill, 2018). We introduce two A2C configurations: a pure quantum and a hybrid quantum classical configuration. We employ VQCs for both the actor and critic components, and evaluate our experiments on the *Cart Pole* control problem from OpenAI gymnasium (Brockman et al., 2016). First, we compare the performance of our quantum A2C configurations with the classical A2C algorithm, ensuring a similar number of parameters. Furthermore, we investigate the effectiveness of a VQC with a classical post-processing layer. Finally, we compare the performance of this hybrid approach with a classical A2C algorithm, maintaining a similar parameter count. This study aims to demonstrate the enhanced learning efficiency and accuracy of quantum A2C algorithms in control tasks with continuous state spaces.

*Authors contributed equally to this work.

Kölle, M., Hgog, M., Ritz, F., Altmann, P., Zorn, M., Stein, J. and Linnhoff-Popien, C.
Quantum Advantage Actor-Critic for Reinforcement Learning.
DOI: 10.5220/0012383900003636

In *Proceedings of the 16th International Conference on Agents and Artificial Intelligence (ICAART 2024) - Volume 1*, pages 297-304
ISBN: 978-989-758-680-4; ISSN: 2184-433X

2 RELATED WORK

Research in QRL has progressed significantly, with studies exploring quantum algorithms and circuits for both policy-based and value-based methods, comparing QRL to classical RL, and applying QRL to real-world problems (Kwak et al., 2021).

Early research introduced VQC for RL, specifically in approximating Q-value functions in Deep Q-Learning (DQN) for discrete and continuous environments (Chen et al., 2019; Skolik et al., 2022). Enhancements like Double DQN were also adapted into VQC architecture, showing efficacy in tasks like robot navigation and in various OpenAI Gym environments (Heimann et al., 2022; Lockwood and Si, 2020).

Significant advancements in policy-based QRL methods have been made, with studies using VQC for algorithms like REINFORCE (Jerbi et al., 2022; Jerbi et al., 2021; Sequeira et al., 2022). In actor-critic methods, VQCs have been effectively used as actor and critic networks. Examples include a policy-VQC for Proximal Policy Optimization and a soft actor-critic algorithm with VQCs outperforming classical models (Kwak et al., 2021; Lan, 2021). Additionally, a quantum version of the A3C algorithm demonstrated superior convergence speed and sample efficiency (Chen, 2023).

Addressing the NISQ era's qubit limitations, studies have combined VQC with neural networks for efficient data processing. Pre-processing neural networks and tensor networks have been employed for dimensionality reduction, while post-processing layers have enhanced VQC's expressive power (Mari et al., 2020; Chen et al., 2021; Chen et al., 2022; Chen, 2023; Sequeira et al., 2022; Hsiao et al., 2022; Meyer et al., 2022a).

3 QUANTUM ADVANTAGE ACTOR-CRITIC

The first step in the A2C algorithm (Line 1) involves initializing both the actor-network $\pi_\theta(s)$ and the critic network $V_\omega(s)$ with random parameters θ and ω. The actor-network maps the current state of the environment to an appropriate action, while the critic network maps the current state to its corresponding state value. Then, initialize the stochastic gradient descent optimizer Adam (Kingma and Ba, 2014) to update the parameters θ and ω throughout the optimization process.

Once the networks have been initialized, the algorithm enters a loop that iterates for each episode. In each iteration t, the algorithm selects an action a_t based on the current state s of the environment, as determined by the actor-network $\pi_\theta(s)$. This action is executed in the environment, and the algorithm observes the resulting reward r_t, the new state s_{t+1}, and the done status d, which indicates whether the episode has ended.

```
Initialize the environment;
Initialize the actor-network π_θ(s);
Initialize the critic-network V_ω(s);
Initialize Adam optimizer for θ and ω;
for each episode do
    Initialize next observation state s_t
     env.reset();
    Initialize done d = False;
    for each iteration t do
        Select an action a_t based on π_θ(s_t);
        Execute action a_t in the environment;
        Observe reward r_t, new state s_{t+1}, and
         done d;
        if d = True then
            break;
        end
        Calculate TD target value
         y = r_t + γV_ω(s_{t+1});
        Calculate advantage A = y − V_ω(s_t);
        Update the actor-network by
         minimizing the loss
         L_actor(θ) = −A log π_θ(a_t);
        Update the critic-network by
         minimizing the loss
         L_critic(ω) = (y − V_ω(s_t))^2;
        Update the state s_t = s_{t+1};
    end
end
```

Algorithm 1: Advantage Actor-Critic Algorithm (Mnih et al., 2016).

The next step is calculating the TD target value y. The advantage A is estimated from the TD error (difference between the TD target value y and the predicted state value). The advantage is then used to update the actor-network by minimizing the loss function $L_{\text{actor}}(\theta)$. and the critic-network $V_\omega(s)$ by minimizing the loss function $L_{\text{critic}}(\omega)$.

Finally, the state s_t of the environment is updated to the new state s_{t+1}, and the algorithm repeats the loop for the next iteration. This process continues until the maximum number of episodes has been reached, or d is set to $True$, at which point the A2C algorithm terminates.

3.1 Baselines

In our study, we compared quantum A2C algorithms with classical A2C implementations using neural networks of varying sizes, ensuring comparable model sizes for a fair analysis. Specifically, we contrasted a classical A2C with four hidden neurons against our quantum A2C, and another with five hidden neurons against our hybrid A2C (Sections 3.2 and 3.3). The neural network architectures, consist of an input layer with four input neurons to encode the 4-dimensional state, a single hidden layer, and an output layer with two neurons for the actor-network and one for the critic network.

The choice of four and five neurons in the hidden layer for the classical A2C models was deliberate, aligning the number of trainable parameters with those in the quantum and hybrid A2C models. This alignment ensures that performance differences are attributable to the inherent characteristics of the models rather than parameter count discrepancies.

For the neural networks' activation functions, we employed the Rectified Linear Unit (ReLU) function (Agarap, 2018) in both actor and critic networks to address the vanishing gradient problem. In the actor-network's output layer, a softmax activation function (Bridle, 1990) was used to generate a probability distribution.

3.2 Quantum Advantage Actor-Critic Algorithm

In this work, we employ a specific VQC architecture, shown in Fig. 1, for both actor and critic quantum circuits in the QA2C and HA2C algorithms. A VQC comprises three main components: an encoding layer, repeated variational layers, and measurements.

The proposed VQC utilizes *RX* quantum gates to encode the observed state of the environment into a quantum state. For the Cart Pole problem, the observed state is four-dimensional, necessitating four qubits in both the actor and critic circuits to represent the state information.

Following the encoding process, a variational layer is applied, repeated a specific number of times n. In this particular implementation, we use $n = 2$ repetitions. Each variational layer consists of four CNOT gates to entangle all qubits and three single-qubit gates, $R_Z(\theta_i)$, $R_Y(\phi_i)$, and $R_Z(\delta_i)$, applied to each qubit i (Kwak et al., 2021). The parameters θ, ϕ, and δ are iteratively optimized using the classical optimization algorithm Adam (Kingma and Ba, 2014).

Lastly, each qubit's state is measured, and the measurement outcomes are utilized to determine the action for the actor and the state value for the critic in the following steps of the A2C algorithm.

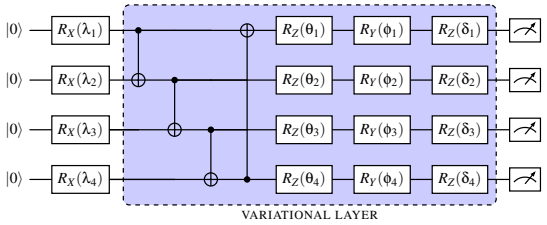

Figure 1: VQC architecture utilized by QA2C and HA2C algorithms.

3.2.1 State Encoding

In this work, the *RX* gate is employed for encoding, which acts on a single qubit and performs a rotation around the x-axis of the Bloch sphere (Nielsen and Chuang, 2010). Given that *RX* rotations are periodic with a period of 2π, different values might map to the same quantum state, leading to inaccurate predictions. To mitigate this issue, additional operations are applied to the observed state variables to ensure the parameters fall within the range of $[-\pi, \pi]$.

The first two variables o_1 and o_2 have finite ranges, whereas the last two variables o_3 and o_4 have infinite ranges. Consequently, we establish separate normalization and transformation rules for these two groups of variables.

For the cart's position o_1 and the pole's angle o_2, which have finite ranges, the normalization procedure consists of simple scaling using their respective minimum and maximum values:

$$\lambda_1 = \frac{\pi}{4.8} o_1, \lambda_2 = \frac{\pi}{0.418} o_2, \tag{1}$$

where λ_1 and λ_2 denote the transformed variables that are input into the quantum circuit.

The normalization process is more intricate than simple scaling for the cart's velocity o_3 and the pole's angular velocity o_4, which have infinite ranges. To normalize these values, we first use the arctan function to map the infinite range to the finite interval $[-\pi/2, \pi/2]$ and then apply simple scaling to stretch the interval to the desired range. The process can be expressed as follows:

$$\lambda_3 = 2 \arctan o_3, \lambda_4 = 2 \arctan o_4 \tag{2}$$

where λ_3 and λ_4 represent the transformed variables used in the quantum circuit.

3.2.2 Measurement and Action Selection of the Quantum Actor

The actor's VQC in the QA2C algorithm is designed to convert the observed state into a quantum state and

predict the optimal action to take. We use a VQC comprising four qubits and two variational layers. At the end of the circuit, the qubits are measured, and the probability of measuring 0 is employed to determine the actor's action. Given that the action space in the Cart Pole environment is two-dimensional, only the measurement values of the first two qubits are considered.

To convert these values into a probability distribution, we apply the softmax function, which maps the input vector (in this case, the probabilities of the first two qubits) to a probability distribution that sums to 1 (Bridle, 1990). The softmax function is defined as:

$$\text{softmax}(x_i) = \frac{e^{x_i}}{\sum_j e^{x_j}} \tag{3}$$

where x_i represents the i-th element of the input vector, e denotes Euler's number, and the sum is taken over all elements in the input vector. After obtaining the probability distribution, the actor selects its action stochastically by randomly choosing an action from the probability distribution, based on the probabilities assigned to each action.

3.2.3 Measurement in Quantum Critic

In the QA2C algorithm, the quantum critic employs a VQC to estimate the value function, which serves as a measure of the quality of a given state for the agent. As only a single value is needed for the estimation, the quantum critic measures just the first qubit and utilizes the probability of measuring 0 as the estimated state value.

3.3 Hybrid Quantum Advantage Actor-Critic Algorithm

In this section, we explore the potential of integrating VQCs and neural networks within the A2C algorithm. Neural networks can be employed in conjunction with VQCs as pre-processing and post-processing layers (Chen, 2023).

In the VQC architecture depicted in Fig. 1, we measured at most two qubits for the actor and one qubit for the critic. With the proposed hybrid architecture, we expand the VQC by incorporating a post-processing neural network layer. This modification allows us to measure all four qubits and scale the VQC output to the desired measurement size. For the actor, we reduce the output from four values to two, corresponding to the action space of the environment. In the case of the critic, we reduce the output from four values to a single value needed for the state value function.

We refer to the proposed architecture as the Hybrid Advantage Actor-Critic (HA2C), which will be applied to the QA2C algorithm in three different approaches. The first approach entails replacing the critic network with a hybrid VQC while retaining the neural network for the actor. The second approach involves substituting the actor-network with a hybrid VQC while keeping the critic as a neural network. Finally, we replace both the actor and critic neural networks with hybrid VQCs.

3.3.1 Hybrid Quantum Actor

The hybrid actor in the HA2C algorithm combines a VQC with a post-processing single-layer neural network, as illustrated in Fig. 2a. The measurements obtained from the VQC are used as inputs for the post-processing layer. The neural network has four inputs and two outputs, enabling the use of measurements from all the qubits, rather than just two, as in the quantum actor in QA2C. The softmax activation function is employed at the neural network output to generate the probability distribution for the actor.

3.3.2 Hybrid Quantum Critic

Similarly, the hybrid critic model comprises a combination of a VQC and a post-processing neural network layer, as depicted in Fig. 2b. The quantum circuit produces measurements that are subsequently used as input for the neural network. The critic's output is a single value, the state function, which means the neural network also has only one output. This setup allows the use of measurements from all four qubits in the VQC to estimate the state value, providing the neural network with a comprehensive set of information to process.

4 EXPERIMENTAL SETUP

This paper investigates the classical A2C algorithm with two distinct implementations, each utilizing two neural networks, as described in Section 3.1 on the CartPole environment. The first implementation employs four neurons in its hidden layer, while the second uses five neurons. Additionally, we examine the quantum versions of A2C, which includes two main architectures: QA2C and HA2C, as explained in Section 3.2 and Section 3.3, respectively. Finally, for both architectures, we present three different actor-critic implementations.

In the first implementation, we replaced the neural network for the critic with a VQC in QA2C and a VQC with post-processing in HA2C, while the actor

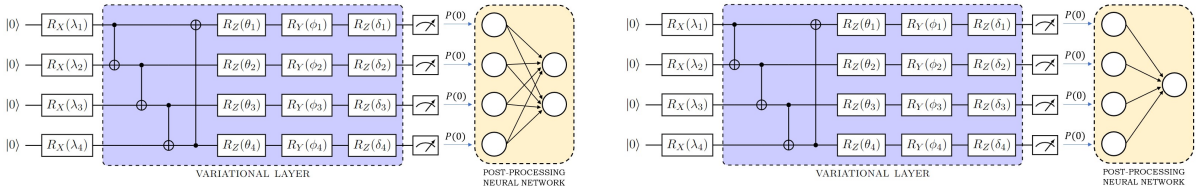

(a) Hybrid VQC used as hybrid actor

(b) Hybrid VQC used as hybrid critic

Figure 2: Hybrid VQC-based hybrid actor and critic models.

remained a neural network. We refer to this as the Advantage Actor-Quantum-Critic (A2Q) algorithm. The second implementation involved using a VQC for the actor in QA2C and a VQC with post-processing in HA2C, while the critic remained a neural network. We refer to this as the Advantage Quantum-Actor-Critic (Q2C) algorithm.

Finally, in the third implementation, we replaced both the actor and critic neural networks with a VQC in QA2C and a VQC with post-processing in HA2C. We refer to this as the Advantage Quantum-Actor-Quantum-Critic (Q2Q) algorithm.

The classical actor and critic in QA2C and HA2C used a neural network with four and five neurons in the hidden layer, respectively. Furthermore, in all experiments, the QA2C and HA2C algorithms were benchmarked against a classical A2C algorithm with four and five neurons in its hidden layer, respectively.

Classical neural networks for actor and critic were implemented using the popular deep learning library PyTorch (Paszke et al., 2019), and we used PennyLane, a widely-used quantum machine learning library, to implement VQCs. The experiments were conducted on the compute cloud provided by Leibniz-Rechenzentrum der Bayerischen Akademie der Wissenschaften (LRZ), which consists of one Intel(R) Xeon(R) Platinum 8160 CPU.

4.1 Cart Pole

The OpenAI-provided Cart Pole environment is a standard benchmark for RL algorithm performance evaluation (Brockman et al., 2016). This environment features a cart moving on a track with a hinged pole. The agent's goal is to prevent the pole from falling by controlling the cart's movement.

The Cart Pole environment is well-suited for testing QRL algorithms due to its simplicity, the challenge of balancing the pole through a series of actions, and a clear reward signal for easy algorithm evaluation and comparison. It involves four state variables representing the cart's position and velocity, and the pole's angle and angular velocity (Gymlibrary, 2022). The continuous nature of these state variables, which can take any real value within a range, adds complexity to the learning process.

In this RL setting, the agent aims to keep the pole upright by moving the cart left or right. Rewards are based on the duration the pole is balanced: positive rewards accumulate each timestep the pole remains upright. Failure occurs if the pole falls (exceeds ±12°) or the cart strays too far from the center (beyond ±2.4), ending the episode (Gymlibrary, 2022). Success is achieved if the pole stays upright for 500 steps, motivating the RL agent to maximize pole balancing duration.

4.2 Hyperparameters and Model Size

Hyperparameters, such as learning rates and discount factors, play a crucial role in determining the performance of RL algorithms (Henderson et al., 2017). Therefore, we conducted a small-scale hyperparameter tuning study to find a suitable learning rate α and discount factor γ for the classical A2C, QA2C, and HA2C algorithms. Based on the results, we selected a learning rate $\alpha = 1 \times 10^{-4}$ to be used in the Adam optimizer and a discount factor $\gamma = 0.99$ for all algorithms. All runs were executed on nodes with Intel(R) Core(TM) i5-4570 CPU @ 3.20GHz.

Our proposed VQC for the QA2C and HA2C algorithms is visualized in Fig. 1. The VQC employs four qubits and two variational layers, with each layer consisting of three single-qubit rotations, resulting in a total of 24 quantum parameters to be optimized. To ensure fair comparisons between the classical A2C and the quantum algorithms, we implemented the A2C algorithm with four and five neurons in the hidden layer.

5 RESULTS

The first experiment aimed to compare the performance of three versions of the QA2C algorithm with the classical A2C algorithm, which had four neurons in the hidden layer. All algorithms were trained on 10 runs, each consisting of 450,000 and 1,000,000 steps

in Fig. 3, respectively. The x-axis denotes the steps, the y-axis shows the average reward obtained for all runs in each step, and the shaded region represents the standard deviation of the results.

The results revealed that none of the proposed quantum architectures, namely A2Q, Q2C, and Q2Q, could learn the Cart Pole environment across all runs. In contrast, classical A2C demonstrated a stable learning curve until a sudden drop at around 400,000 steps reaching a reward of 73. However, the reward threshold for the Cart Pole environment is 475, which the classical A2C's average reward did not attain, indicating its inability to solve the environment across all runs.

The goal of the second experiment was to improve the architecture of the VQC by combining it with a post-processing neural network in order to achieve better results. Fig. 3 shows the performance of the classical A2C with 5 neurons in the hidden layer and the three versions of the HA2C algorithm: HA2Q, HQ2C, and HQ2Q.

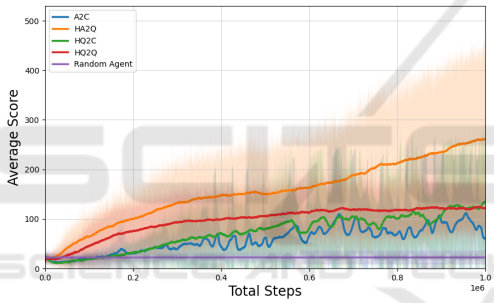

Figure 3: HA2C and classical A2C performance in Cart Pole.

The aim was to train both algorithms on 10 runs, each with 1,000,000 steps in the Cart Pole environment. In Fig. 3, we can see an evident success for the HA2C algorithms over classical A2C, especially in HA2Q and HQ2Q. The proposed hybrid architecture learned the task in almost every run, while the classical A2C succeeded in only 5 of the 10 runs. Two additional VQCs with different single-qubit rotations were also tested in a pre-study for the QA2C and HA2C algorithms. However, the other QA2C algorithms also failed to learn.

In conclusion, the experiments demonstrated that the hybrid quantum-classical approach could achieve better results than the classical A2C algorithm with 5 neurons in the hidden layer. Specifically, the HA2C algorithms, HA2Q and HQ2Q, showed significant improvement over the classical A2C algorithm, learning the Cart Pole environment in almost every run. This highlights the potential of combining quantum and classical architectures to enhance the performance of reinforcement learning algorithms.

However, it is essential to consider the significantly longer training time for the quantum algorithms compared to the classical A2C algorithm. This performance gap emphasizes the need for further research and optimization of quantum algorithms to reduce training time and improve their applicability in real-world scenarios.

Future work could involve exploring alternative quantum architectures or optimization methods to enhance performance and reduce training time. Additionally, more complex environments and tasks could be considered to further investigate the potential of quantum-classical hybrid approaches in reinforcement learning.

5.1 Discussion

After conducting experiments on the Cart Pole environment, it became evident that the pure quantum A2C algorithm did not effectively learn the task. After looking at the average gradients (-0.000056), we concluded that this was caused by vanishing gradients. Both hybrid approaches, A2Q and Q2C suffer from the same problem using the quantum actor and quantum critic. Additionally, like with any machine learning algorithm, the performance of VQCs can be influenced by several factors, including hyperparameter settings, circuit structure, and task complexity. To improve the performance of the quantum algorithm, future work could explore techniques such as circuit ansatz design or gradient-free optimization to mitigate this issue (McClean et al., 2018; Chen et al., 2022). In summary, the quantum approach did not provide any significant advantage over classical methods.

Building upon that, we employ VQCs with classical post-processing to circumvent barren plateaus. This proved to be more effective in addressing the challenges of the Cart Pole environment than the classical A2C algorithm, as the hybrid quantum A2C substantially outperforms the classical A2C in learning the environment. The VQC uses a post-processing neural network, which may be crucial for enabling the VQC to learn. Notably, both HA2Q and HQ2C started to learn the task immediately, while HQ2Q learned at a slower rate.

These experiments were conducted on a quantum simulator since current quantum hardware is not widely available at the time of writing. This circumstance leads to significantly higher training times for all tested quantum approaches than the classical baseline. Thus, without access to an actual quantum device, there is currently no real benefit to the quantum

approaches. Even with exclusive access to real quantum hardware, we can not say for certain if a quantum parameter trains as fast as a classical one. It is essential to recognize that the field of quantum computing and quantum machine learning is still in its early stages, with much research needed to gain a deeper understanding of the capabilities and limitations of VQCs in machine learning. As such, further exploration is necessary to unlock the full potential of this emerging technology.

6 CONCLUSION

We investigated how quantum computing techniques could enhance the performance of the A2C algorithm. To achieve this goal, we conducted experiments and compared the performance of three variations of the A2C algorithm: classical, quantum, and hybrid A2C. In each variation, we replaced either the actor, critic, or both with a quantum circuit, leading to a total of three different configurations. By testing these configurations, we aimed to understand the impact of each variation on the algorithm's overall performance. Furthermore, ensuring a fair comparison between the algorithms was a significant challenge in this study. Therefore, to maintain fairness, we kept the number of parameters in the algorithms roughly equal.

Our results show that the classical A2C outperforms the pure quantum A2C. To improve the quantum A2C performance, we introduced a hybrid approach integrating a VQC with a post-processing neural network layer. We tested three configurations of the hybrid algorithm and found that it substantially outperformed both the quantum and classical counterparts. This paper contributes to the growing body of evidence highlighting the potential of combining quantum computing and classical machine learning algorithms to improve reinforcement learning tasks' performance.

Future research in RL and QRL is essential, particularly in hyperparameter tuning, which is vital for optimizing performance. Exploring various VQC architectures, including data re-uploading, not used in our current models, could enhance performance (Pérez-Salinas et al., 2020). Investigating different encoding strategies like amplitude encoding (Schuld and Petruccione, 2018), and employing techniques like weight re-mapping (Kölle et al., 2023) could improve convergence.

ACKNOWLEDGEMENTS

This research is part of the Munich Quantum Valley, which is supported by the Bavarian state government with funds from the Hightech Agenda Bayern Plus.

REFERENCES

Agarap, A. F. (2018). Deep learning using rectified linear units (relu). *arXiv preprint arXiv:1803.08375*.

Andrychowicz, M., Raichuk, A., Stańczyk, P., Orsini, M., Girgin, S., Marinier, R., Hussenot, L., Geist, M., Pietquin, O., Michalski, M., et al. (2021). What matters for on-policy deep actor-critic methods? a large-scale study. In *International conference on learning representations*.

Bauer, B., Bravyi, S., Motta, M., and Chan, G. K.-L. (2020). Quantum Algorithms for Quantum Chemistry and Quantum Materials Science. *Chemical Reviews*, 120(22):12685–12717. Publisher: American Chemical Society.

Biamonte, J., Wittek, P., Pancotti, N., Rebentrost, P., Wiebe, N., and Lloyd, S. (2017). Quantum machine learning. *Nature*, 549(7671):195–202.

Bridle, J. S. (1990). Probabilistic interpretation of feedforward classification network outputs, with relationships to statistical pattern recognition. In Soulié, F. F. and Hérault, J., editors, *Neurocomputing*, pages 227–236, Berlin, Heidelberg. Springer Berlin Heidelberg.

Brockman, G., Cheung, V., Pettersson, L., Schneider, J., Schulman, J., Tang, J., and Zaremba, W. (2016). Openai gym. *arXiv preprint arXiv:1606.01540*.

Cao, Y., Romero, J., Olson, J. P., Degroote, M., Johnson, P. D., Kieferová, M., Kivlichan, I. D., Menke, T., Peropadre, B., Sawaya, N. P. D., Sim, S., Veis, L., and Aspuru-Guzik, A. (2019). Quantum chemistry in the age of quantum computing. *Chemical Reviews*, 119(19):10856–10915.

Cerezo, M., Arrasmith, A., Babbush, R., Benjamin, S. C., Endo, S., Fujii, K., McClean, J. R., Mitarai, K., Yuan, X., Cincio, L., and Coles, P. J. (2020). Variational quantum algorithms. *Nature Reviews Physics*, 3:625 – 644.

Chen, S. Y.-C. (2023). Asynchronous training of quantum reinforcement learning.

Chen, S. Y.-C., Huang, C.-M., Hsing, C.-W., Goan, H.-S., and Kao, Y.-J. (2022). Variational quantum reinforcement learning via evolutionary optimization. *Machine Learning: Science and Technology*, 3(1):015025.

Chen, S. Y.-C., Huang, C.-M., Hsing, C.-W., and Kao, Y.-J. (2021). An end-to-end trainable hybrid classical-quantum classifier. *Machine Learning: Science and Technology*, 2(4):045021.

Chen, S. Y.-C., Yang, C.-H. H., Qi, J., Chen, P.-Y., Ma, X., and Goan, H.-S. (2019). Variational quantum circuits for deep reinforcement learning.

Dral, P. O. (2020). Quantum Chemistry in the Age of Machine Learning. *The Journal of Physical Chemistry Letters*, 11(6):2336–2347. Publisher: American Chemical Society.

Farhi, E., Goldstone, J., and Gutmann, S. (2014). A Quantum Approximate Optimization Algorithm. *arXiv:1411.4028 [quant-ph]*. arXiv: 1411.4028.

Farhi, E. and Harrow, A. W. (2016). Quantum supremacy through the quantum approximate optimization algorithm.

Gymlibrary, F. F. (2022). Cart pole - gym documentation.

Heimann, D., Hohenfeld, H., Wiebe, F., and Kirchner, F. (2022). Quantum deep reinforcement learning for robot navigation tasks.

Henderson, P., Islam, R., Bachman, P., Pineau, J., Precup, D., and Meger, D. (2017). Deep reinforcement learning that matters.

Hsiao, J.-Y., Du, Y., Chiang, W.-Y., Hsieh, M.-H., and Goan, H.-S. (2022). Unentangled quantum reinforcement learning agents in the openai gym.

Jerbi, S., Cornelissen, A., Ozols, M., and Dunjko, V. (2022). Quantum policy gradient algorithms.

Jerbi, S., Gyurik, C., Marshall, S. C., Briegel, H. J., and Dunjko, V. (2021). Parametrized quantum policies for reinforcement learning.

Kingma, D. P. and Ba, J. (2014). Adam: A method for stochastic optimization.

Kober, J., Bagnell, J. A., and Peters, J. (2013). Reinforcement learning in robotics: A survey. *The International Journal of Robotics Research*, 32(11):1238–1274.

Konda, V. and Tsitsiklis, J. (1999). Actor-critic algorithms. In Solla, S., Leen, T., and Müller, K., editors, *Advances in Neural Information Processing Systems*, volume 12. MIT Press.

Kwak, Y., Yun, W. J., Jung, S., Kim, J.-K., and Kim, J. (2021). Introduction to quantum reinforcement learning: Theory and pennylane-based implementation.

Kölle, M., Giovagnoli, A., Stein, J., Mansky, M. B., Hager, J., and Linnhoff-Popien, C. (2023). Improving convergence for quantum variational classifiers using weight re-mapping.

Lan, Q. (2021). Variational quantum soft actor-critic.

Lockwood, O. and Si, M. (2020). Reinforcement learning with quantum variational circuits.

Mari, A., Bromley, T. R., Izaac, J., Schuld, M., and Killoran, N. (2020). Transfer learning in hybrid classical-quantum neural networks. *Quantum*, 4:340.

McClean, J. R., Boixo, S., Smelyanskiy, V. N., Babbush, R., and Neven, H. (2018). Barren plateaus in quantum neural network training landscapes. *Nature Communications*, 9(1).

Meyer, N., Scherer, D. D., Plinge, A., Mutschler, C., and Hartmann, M. J. (2022a). Quantum policy gradient algorithm with optimized action decoding.

Meyer, N., Ufrecht, C., Periyasamy, M., Scherer, D. D., Plinge, A., and Mutschler, C. (2022b). A survey on quantum reinforcement learning.

Mnih, V., Badia, A. P., Mirza, M., Graves, A., Harley, T., Lillicrap, T. P., Silver, D., and Kavukcuoglu, K. (2016). Asynchronous methods for deep reinforcement learning. In *Proceedings of the 33rd International Conference on International Conference on Machine Learning - Volume 48*, ICML'16, page 1928–1937. JMLR.org.

Nielsen, M. and Chuang, I. (2010). *Quantum Computation and Quantum Information: 10th Anniversary Edition*. Cambridge University Press.

Paszke, A., Gross, S., Massa, F., Lerer, A., Bradbury, J., Chanan, G., Killeen, T., Lin, Z., Gimelshein, N., Antiga, L., Desmaison, A., Kopf, A., Yang, E., DeVito, Z., Raison, M., Tejani, A., Chilamkurthy, S., Steiner, B., Fang, L., Bai, J., and Chintala, S. (2019). Pytorch: An imperative style, high-performance deep learning library. In *Advances in Neural Information Processing Systems 32*, pages 8024–8035. Curran Associates, Inc.

Pérez-Salinas, A., Cervera-Lierta, A., Gil-Fuster, E., and Latorre, J. I. (2020). Data re-uploading for a universal quantum classifier. *Quantum*, 4:226.

Pirandola, S., Andersen, U. L., Banchi, L., Berta, M., Bunandar, D., Colbeck, R., Englund, D., Gehring, T., Lupo, C., Ottaviani, C., Pereira, J. L., Razavi, M., Shaari, J. S., Tomamichel, M., Usenko, V. C., Vallone, G., Villoresi, P., and Wallden, P. (2020). Advances in quantum cryptography. *Advances in Optics and Photonics*, 12(4):1012.

Preskill, J. (2018). Quantum computing in the NISQ era and beyond. *Quantum*, 2:79.

Schuld, M. and Petruccione, F. (2018). *Supervised Learning with Quantum Computers*. Springer Publishing Company, Incorporated, 1st edition.

Sequeira, A., Santos, L. P., and Barbosa, L. S. (2022). Policy gradients using variational quantum circuits.

Shor, P. W. (1997). Polynomial-time algorithms for prime factorization and discrete logarithms on a quantum computer. *SIAM Journal on Computing*, 26(5):1484–1509.

Silver, D., Schrittwieser, J., Simonyan, K., Antonoglou, I., Huang, A., Guez, A., Hubert, T., Baker, L., Lai, M., Bolton, A., Chen, Y., Lillicrap, T., Hui, F., Sifre, L., van den Driessche, G., Graepel, T., and Hassabis, D. (2017). Mastering the game of Go without human knowledge. *Nature*, 550(7676):354–359. Bandiera_abtest: a Cg_type: Nature Research Journals Number: 7676 Primary_atype: Research Publisher: Nature Publishing Group Subject_term: Computational science;Computer science;Reward Subject_term_id: computational-science;computer-science;reward.

Skolik, A., Jerbi, S., and Dunjko, V. (2022). Quantum agents in the gym: a variational quantum algorithm for deep q-learning. *Quantum*, 6:720.

You, Y., Pan, X., Wang, Z., and Lu, C. (2017). Virtual to real reinforcement learning for autonomous driving. *CoRR*, abs/1704.03952.